INVOLVEMENT OF MICROTUBULES AND 10-NM FILAMENTS IN THE MOVEMENT AND POSITIONING OF NUCLEI IN SYNCYTIA

EUGENIA WANG, RISE K. CROSS, and PURNELL W. CHOPPIN

From The Rockefeller University, New York 10021

ABSTRACT

Previous studies (Holmes, K. V., and P. W. Choppin. *J. Exp. Med.* **124**:501–520; *J. Cell Biol.* **39**:526–543) showed that infection of baby hamster kidney (BHK21-F) cells with the parainfluenza virus SV5 causes extensive cell fusion, that nuclei migrate in the syncytial cytoplasm and align in tightly-packed rows, and that microtubules are involved in nuclear movement and alignment. The role of microtubules, 10-nm filaments, and actin-containing microfilaments in this process has been investigated by immunofluorescence microscopy using specific antisera, time-lapse cinematography, and electron microscopy. During cell fusion, microtubules and 10-nm filaments from many cells form large bundles which are localized between rows of nuclei. No organized bundles of actin fibers were detected in these areas, although actin fibers were observed in regions away from the aligned nuclei. Although colchicine disrupts microtubules and inhibits nuclear movement, cytochalasin B (CB; 20–50 μg/ml) does not inhibit cell fusion or nuclear movement. However, CB alters the shape of the syncytium, resulting in long filamentous processes extending from a central region. When these processes from neighboring cells make contact, fusion occurs, and nuclei migrate through the channels which are formed. Electron and immunofluorescence microscopy reveal bundles of microtubules and 10-nm filaments in parallel arrays within these processes, but no bundles of microfilaments were detected. The effect of CB on the structural integrity of microfilaments at this high concentration (20 μg/ml) was demonstrated by the disappearance of filaments interacting with heavy meromyosin. Cycloheximide (20 μg/ml) inhibits protein synthesis but does not affect cell fusion, the formation of microtubules and 10-nm filament bundles, or nuclear migration and alignment; thus, continued protein synthesis is not required. The association of microtubules and 10-nm filaments with nuclear migration and alignment suggests that microtubules and 10-nm filaments are two components in a system which serves both cytoskeletal and force-generating functions in intracellular movement and position of nuclei.

KEY WORDS cell fusion · cytochalasin B · immunofluorescence microscopy · microfilaments · simian virus 5

Previous studies from this laboratory showed that infection of monolayers of baby hamster kidney (BHK21-F) cells with the parainfluenza virus, sim-

J. CELL BIOLOGY © The Rockefeller University Press · 0021-9525/79/11/0320/18 $1.00
Volume 83 November 1979 320–337

ian virus 5 (SV5), causes rapid and extensive cell fusion, with most cells being incorporated into a giant syncytium within 14–24 h after infection (10, 24, 25). Nuclei were observed to move through the syncytial cytoplasm, and to become aligned in tightly packed parallel rows (24, 25). Electron microscopy showed that there were bundles of microtubules and filaments ~80 Å in diameter (now referred to as 10-nm filaments) parallel to and between the rows of nuclei. Nuclear migration and alignment was abolished by treatment with colchicine which disrupted the microtubules. It was concluded at that time that microtubules were involved in the positioning and movement of nuclei within the cytoplasm, that microtubules demarcated cytoplasmic channels through which the nuclei migrated, and that they might be involved in the mechanism of nuclear movement (25).

In addition to microtubules, two other cytoplasmic fibers, microfilaments and 10-nm filaments (also known as intermediate filaments), have also been implicated in various aspects of cell motility (3, 17–19, 36, 43, 54). Microfilaments have been found to represent the nonmuscle actomyosin-like machinery responsible for such motile activities as membrane ruffling, cell locomotion, cytokinesis, nerve axonal outgrowth, and micro- and macropinocytosis (3, 18, 28, 33, 41, 47, 56, 57). Although earlier studies suggested a similarity in composition between microtubules and 10-nm filaments, recent structural and chemical studies have demonstrated that they are distinct. Microtubules and 10-nm filaments have been consistently found together in BHK21 cells (18, 19, 25, 54) and in nerve axons (35, 43, 57). It was therefore of interest to extend the earlier studies from this laboratory which demonstrated an association of microtubules with nuclear movements and aligment in SV5-infected BHK21-F syncytia, to an examination of the role in such movement of all three cytoplasmic fibers, i.e, microtubules, microfilaments, and 10-nm filaments. This communication describes the role of organized bundles of microtubules and 10-nm filaments in nuclear movement. No evidence was found for the involvement of actin-containing fibers, but the involvement of actin not organized into fibers or bundles cannot be excluded. These results suggest that microtubules and 10-nm filaments are two components of a system which may play a role in both cytoskeletal and force-generating functions in the intracellular movement and positioning of nuclei and other cellular components.

These studies have been presented in part at the Cold Spring Harbor Meeting on the Cytoskeleton, 17–21 May 1978, and the 1978 Meeting of the American Society for Cell Biology (52).

MATERIALS AND METHODS

Cell Cultures

BHK21-F cells, a subline of the original BHK21-13 cell line derived by Stoker and Macpherson (50), were grown either in 100-mm plastic Petri dishes (Falcon Labware, Div. of Becton, Dickinson & Co., Oxnard, Calif.) or on glass coverslips (No. 1) in reinforced Eagle's medium (REM) containing 10% calf serum and 10% tryptose phosphate broth as described previously (24). Monolayers of the CV-1 line of African green monkey kidney cells, clone TC-7 (13), were grown in REM with 10% fetal calf serum. Cultures were maintained in an incubator at 37°C in a humidified atmosphere of 95% air-5% CO_2.

Virus Inoculation

The growth of the W3 strain of SV5 (9) has been described in detail previously (24). Confluent BHK21-F cultures were washed with phosphate-buffered saline (PBS, pH 7.2), and inoculated with ~1–5 infective virus particles (PFU)/cell. Adsorption was carried out for 2 h at 37°C, the inoculum removed, and fresh REM added; cultures were then incubated at 37°C.

Under these conditions, cell fusion and nuclear migration and alignment usually occur in 18–24 h. To induce more synchronous cell fusion, in some experiments after virus adsorption at 37°C, the infected cells were maintained at 33°C for ~12 h and then shifted to 39.5°C. Very little cell fusion occurred during incubation at 33°C; however, immediately after the shift to 39.5°C, rapid fusion began and the process of syncytial formation and nuclear movement and alignment was complete ~4–6 h after the temperature shift. This provided a shortened period of activity which could be monitored by microscopy.

Light Microscopy

Cells were grown on coverslips in the bottom of 35-mm plastic Petri dishes. After the cells had attached firmly, the coverslips were mounted cell side down on 3 × 1-in^2 glass slides, with pieces of coverslip placed between the coverslips and slide to avoid crushing the cells. A mixture of paraffin, petroleum jelly, and lanolin (1:1:1 by weight) was used to seal the four edges of the coverslip. A Sage air curtain incubator (Sage Instruments Div., Orion Research Inc., Cambridge, Mass.) was used to maintain the temperature at 37° or 39.5°C. The cultures were observed with a Zeiss Photomicroscope III (Carl Zeiss, Inc., New York) equipped with phase-contrast, polarized-light, and epifluorescence optics. Observations were recorded on 35-mm Tri-X Kodak film.

Indirect Immunofluorescence

A detailed description of the preparation of antibody and the processing of samples for indirect immunofluorescence microscopy have been described previously (48). Briefly, formaldehyde-fixed and acetone-treated cells were incubated first with various rabbit immune sera, and then with fluorescein-conjugated goat antibody against rabbit globulin. Labeled cells were examined with a No. 53 barrier filter, fluorescein isothiocyanate (FITC) excitation filter, and a planapochromat 63/1.5 objective with an

epifluorescence light source. Fluorescent images were recorded on Kodak Tri-X 35-mm film.

Isolation and purification of tubulin was performed according to the method of Shelanski and Taylor (42). Native 6 S tubulin was used as the immunogen for the production of antiserum in rabbits. Purified 6 S tubulin (4 mg) was mixed with complete Freund's adjuvant and injected i.m. 6 wk later, a second i.v. injection of 400 μg of antigen was administered. Approx. 7–10 d after a second injection, antibodies against tubulin could be detected by immunodiffusion. A single band of antigen and antibody complex was observed on an Ouchterlony plate. A high titer of antiserum against tubulin could be detected by using a large amount of immunogen in the initial injection. The specificity of the serum for microtubules was shown by staining cells with either preimmune serum or immune serum absorbed with purified 6 S tubulin (Fig. 1 *a–d*); in neither case was staining of microtubule networks or spindle fibers observed.

Antiserum against 10-nm filaments of BHK21 cells was the

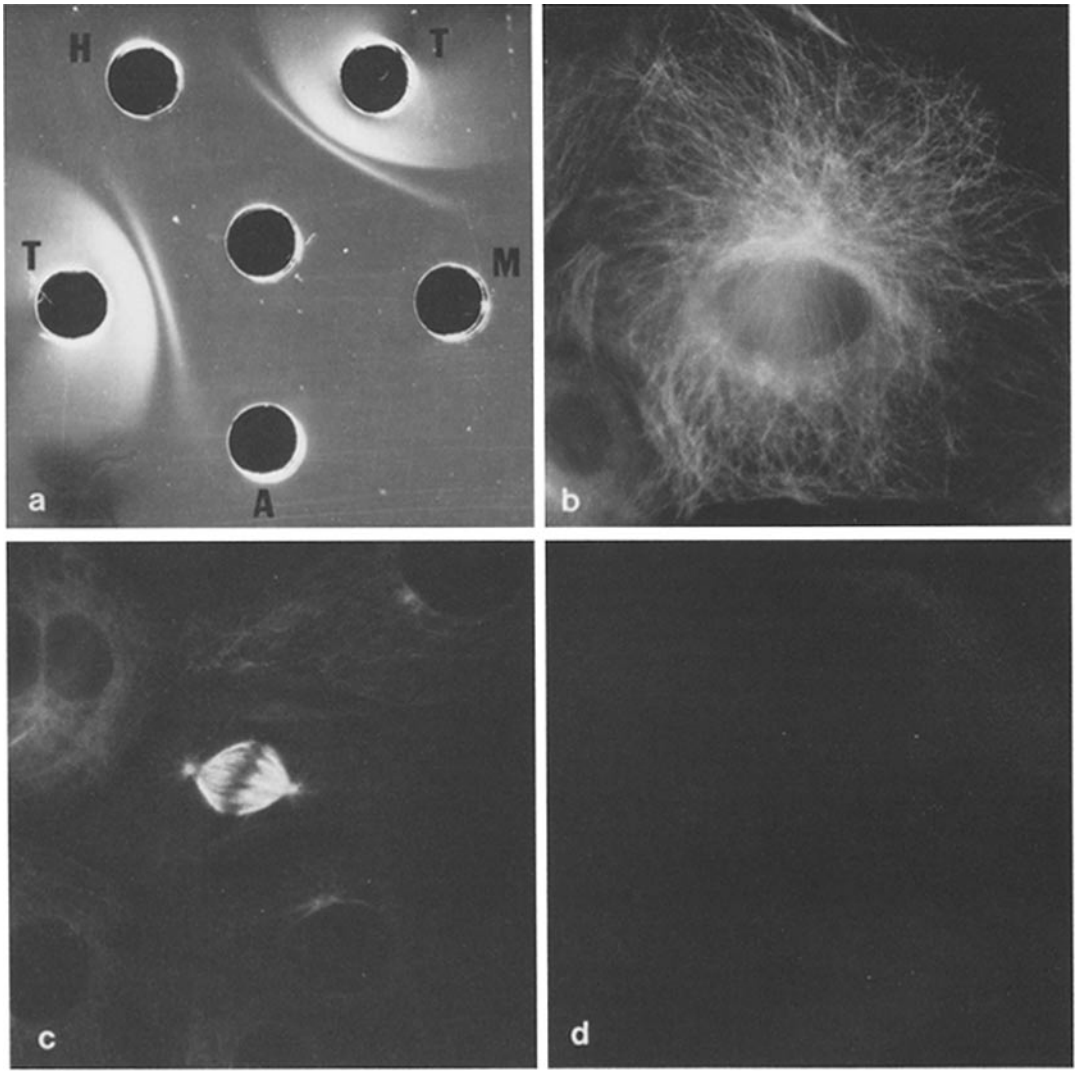

FIGURE 1 Demonstration of the specificity of antiserum against tubulin in BHK21-F and CV-1 cells. × 950. (*a*) Immunodiffusion of purified 6S tubulin (*T*), myosin (*M*), actin (*A*), and the high molecular weight protein of microtubules (*H*) against antiserum to tubulin placed in the center well. Precipitation occurred only with tubulin. A 1:10 dilution of antiserum and 0.5 mg/ml of purified proteins were used. Diffusion was in 0.6% agarose in PBS, pH 7.2. (*b*) Immunofluorescence staining of BHK21-F cells with antitubulin. (*c*) Staining of spindle fibers of BHK21-F cells with antitubulin. (*d*) Lack of staining of BHK21-F cells with immune serum preadsorbed with purified tubulin.

generous gift of Doctors Robert D. Goldman and Judith Starger. The specificity of this antiserum was documented in their report (48).

The organization and distribution of actin in SV5-infected BHK21 syncytia was examined by fluorescence microscopy by incubation with either deoxyribonuclease I (DNase I) and antiserum to DNase I or with labeled heavy meromyosin (HMM). The specific interaction of DNase I and cellular actin and the specificity of applying this method to visualize actin distribution were reported earlier (53). The staining procedure involving the use of biotinyl-HMM in combination with fluorescein-avidin was carried out according to the report of Heggeness and Ash (22), and the reagents for HMM staining were the generous gift of Dr. Heggeness.

Time-lapse Cinematography

The process of cell fusion and nuclear movement and alignment in SV5-infected BHK21-F cells was photographed as previously described (25). Most of the observations were recorded on 16-mm Plus-X Kodak movie film.

Electron Microscopy

Culture cells were fixed for 30 min in Petri dishes at room temperature in 1% glutaraldehyde in PBS. After a brief rinse with PBS, the cells were postfixed for 30 min in a 1% solution of OsO_4 in the same buffer. Cells were then rinsed twice, dehydrated rapidly through a graded series of alcohols, and flat-embedded in Epon 812 (30). Polymerized Epon was broken apart from the Petri dish by applying mechanical pressure. Epon-embedded cells of interest were selected with a Zeiss inverted microscope and cut from the main block of plastic with a punch mounted in a drill press. The resulting small blocks were remounted for thin sectioning parallel to the substrate side of the cell. Sections were cut with a diamond knife on a Sorvall-Porter-Blum MT-2 microtome (DuPont Instruments-Sorvall, DuPont Co., Newtown, Conn.), and were mounted on parlodion-carbon-coated copper grids. These were stained with hot uranyl acetate (29) and lead citrate (38). Electron microscope observations were made with a Philips 300 electron microscope.

Preparation of HMM and Glycerinated Models

HMM was prepared by the methods of Szent-Györgi (51) and Pollard et al. (37). Glycerination was carried out according to Chang and Goldman (8). SV5-infected BHK21-F syncytia were treated with 50, 25, 12.5, and 5% glycerol in standard salt solution (0.05 M KCl, 0.005 M $MgCl_2$, and 0.006 M potassium phosphate buffer [pH 7.0]) for 30 min each at room temperature. Cultures were then reacted with rabbit HMM in 5% glycerol for 30 min. Controls were incubated simultaneously in buffered 5% glycerol solution without HMM. An HMM-sodium pyrophosphate mixture was used as an additional control to test the dissociation of actin-HMM complex (15). Cells were then processed for electron microscopy as described.

RESULTS

BHK21-F cells are fibroblastic and are usually spindle-shaped and oriented in parallel arrays in a confluent monolayer (50). Observation of uninfected cells by indirect immunofluorescence microscopy using antiserum to tubulin indicated that the microtubules were distributed in longitudinal arrays (Fig. 2 *a*). A similar parallel arrangement of 10-nm filaments was also observed using fluorescent antiserum against these structures (Fig. 2 *b*).

Fig. 3 *a* shows the alignment of nuclei in a large multinucleated syncytium 24 h after infection with the parainfluenza virus SV5. As described previously, the nuclei in these syncytia migrate over long distances to form these tightly packed parallel rows in the syncytial cytoplasm (10, 24, 25). Electron microscopy reveals 24-nm microtubules and 10- to 12-nm filaments oriented parallel to the

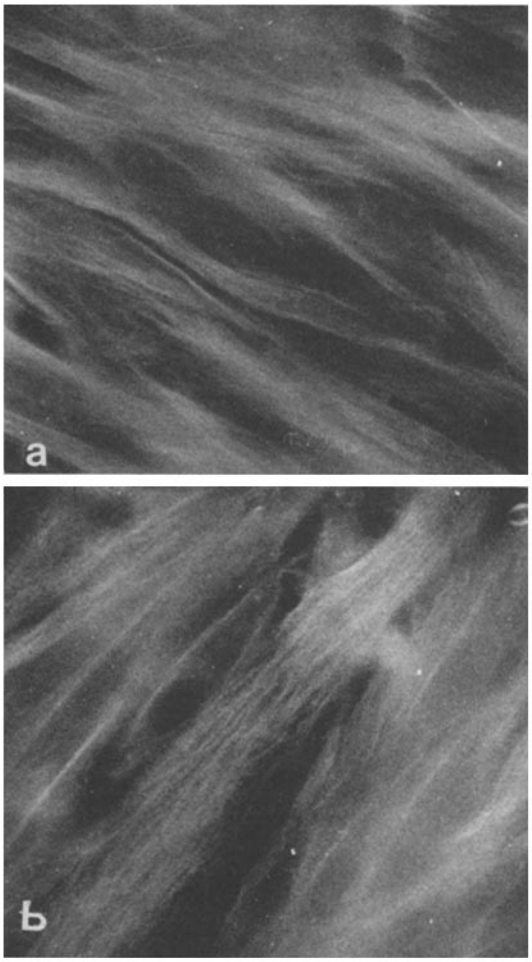

FIGURE 2 Light micrographs of uninfected BHK21-F cell monolayer cultures. × 810. (*a*) Immunofluorescence micrograph using antiserum against calf brain tubulin. (*b*) Immunofluorescence micrograph using antiserum against 10-nm filament protein of BHK21-F cells.

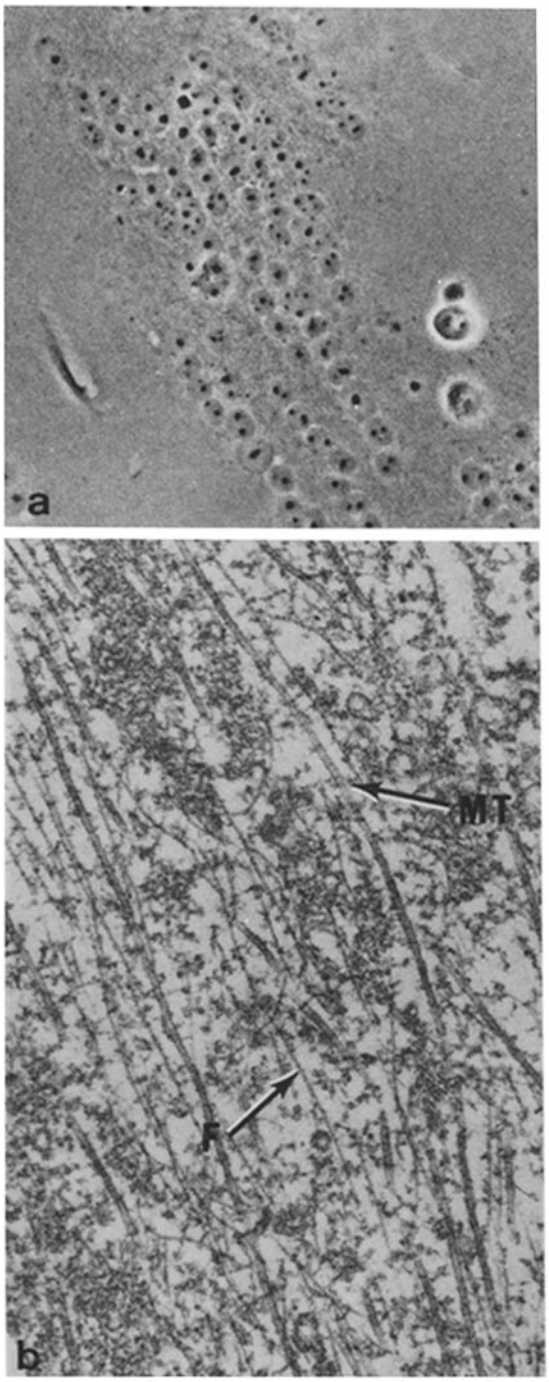

FIGURE 3 (*a*) Phase-contrast micrograph of an SV5-induced BHK21-F syncytium. × 400. (*b*) Electron micrograph of an area between aligned nuclei. Note the parallel arrangement of microtubules and 10-nm filaments. Microtubule (*MT*); 10-nm filament (*F*). × 67,500.

rows of nuclei (25; Fig. 3*b*). Previous studies have shown that colchicine disrupts these microtubules as well as the migration and alignment of the nuclei in the syncytial cytoplasm (25). These earlier observations suggested a possible function of microtubules in directing nuclear movement and perhaps in providing the motive force for such movement.

The role of microtubules in nuclear motility was explored further by indirect immunofluorescence microscopy using antiserum to tubulin. The availability of specific antiserum to 10-nm filaments also permitted us to examine these fibrous structures, which have recently been implicated in various aspects of cell motility (17, 20, 48, 49, 54), to determine their possible involvement in nuclear movement and force generation. As shown in Fig. 4*a*, a phase-dense area which contains a large number of filamentous structures is found between aligned rows of nuclei. Immunofluorescence microscopy using antiserum against tubulin revealed that these phase-dense areas contained microtubules organized in large bundles (Fig. 4*b*) which appear to be formed by the aggregation of large numbers of individual microtubules (Fig. 4*c*). Antiserum against 10-nm filaments demonstrated that these fibrous structures also formed large bundles in the same phase-dense area between nuclei (Fig. 4*d*). Individual filaments were also seen aggregated into large bundles immediately outside the nuclear region (Fig. 4*e*). This bundle formation of microtubules and 10-nm filaments was observed in the area of the clustered and aligned nuclei. As described previously (24, 25), essentially all of the nuclei in the syncytia participate in movement in the cytoplasm, and such movement usually results in the alignment of all nuclei in parallel rows. Consistent with this observation, microtubules and 10-nm filament bundles were always observed next to aligned nuclei. Rows of nuclei without bundles of tubules and filaments adjacent to them were not found, and large bundles in areas other than near nuclei were rarely seen. As shown in Fig. 4*f*, 10-nm filaments appeared randomly distributed in the syncytial cytoplasm away from the perinuclear region.

Because of the large size of these fibrous bundles, a more detailed study of their morphogenesis was undertaken using polarized-light and phase-contrast optics. As described in Materials and Methods, infected cultures were incubated overnight at 33°C, shifted to 39.5°C, and then directly monitored using a Sage incubator. Cell fusion,

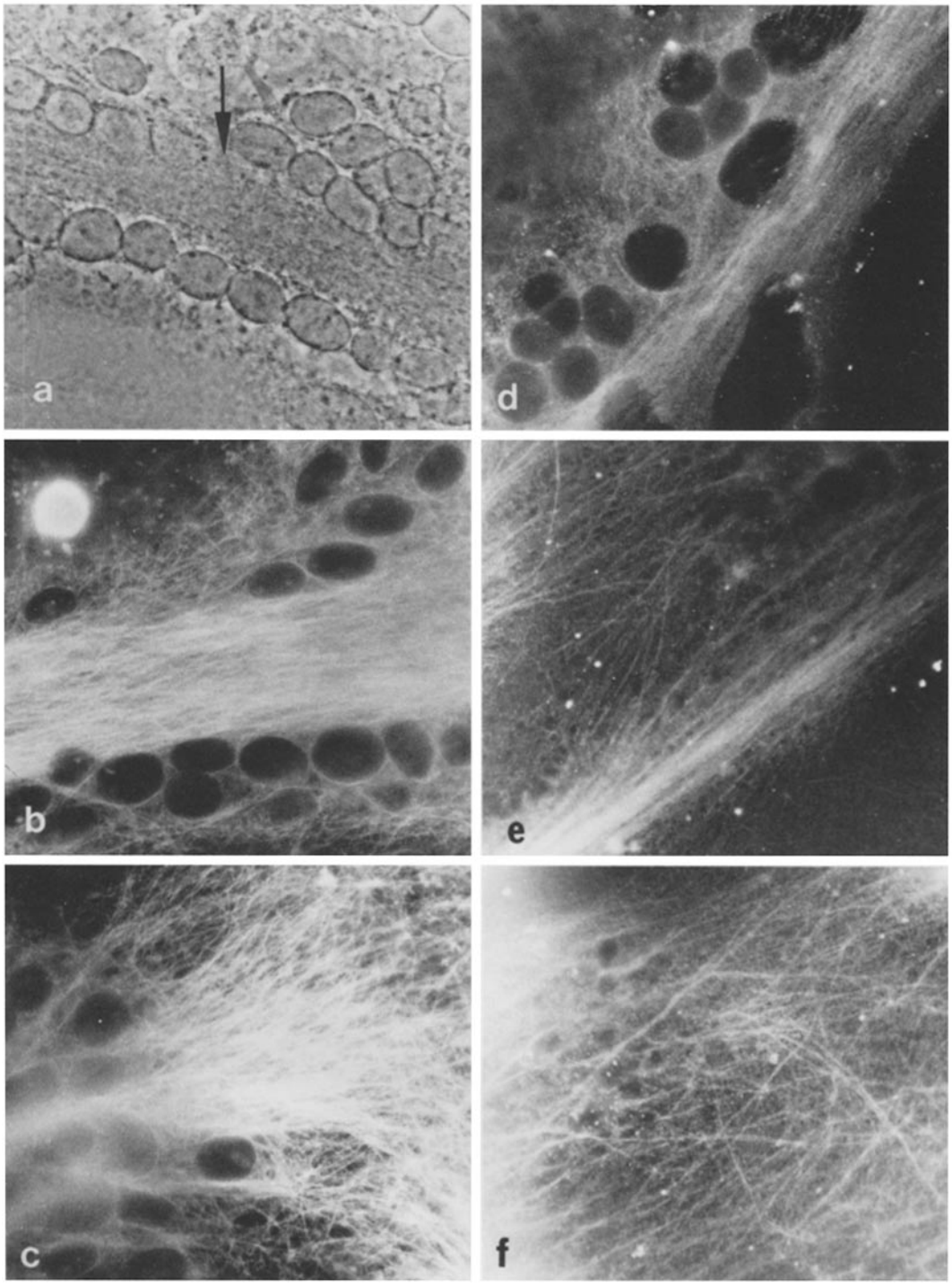

FIGURE 4 Light micrographs of microtubule and 10-nm filament organization in SV5-infected BHK21-F syncytia. Cultures were infected at 37°C, fixed, and acetone-treated for immunofluorescence microscopy at ~24 h after infection. × 750. (*a*) Phase-contrast micrograph of a phase-dense area between aligned nuclei (arrow). (*b–f*) Immunofluorescence micrographs using antiserum to microtubules or 10-nm filaments. (*b*) Microtubules in an area similar to that shown in *a*. (*c*) Aggregation of individual microtubules into large bundles. (*d*) 10-nm filaments within an area similar to that in *a*. (*e*) Aggregation of individual 10-nm filaments into large bundles. (*f*) Disorganized pattern of 10-nm filaments in an area not associated with aligned nuclei.

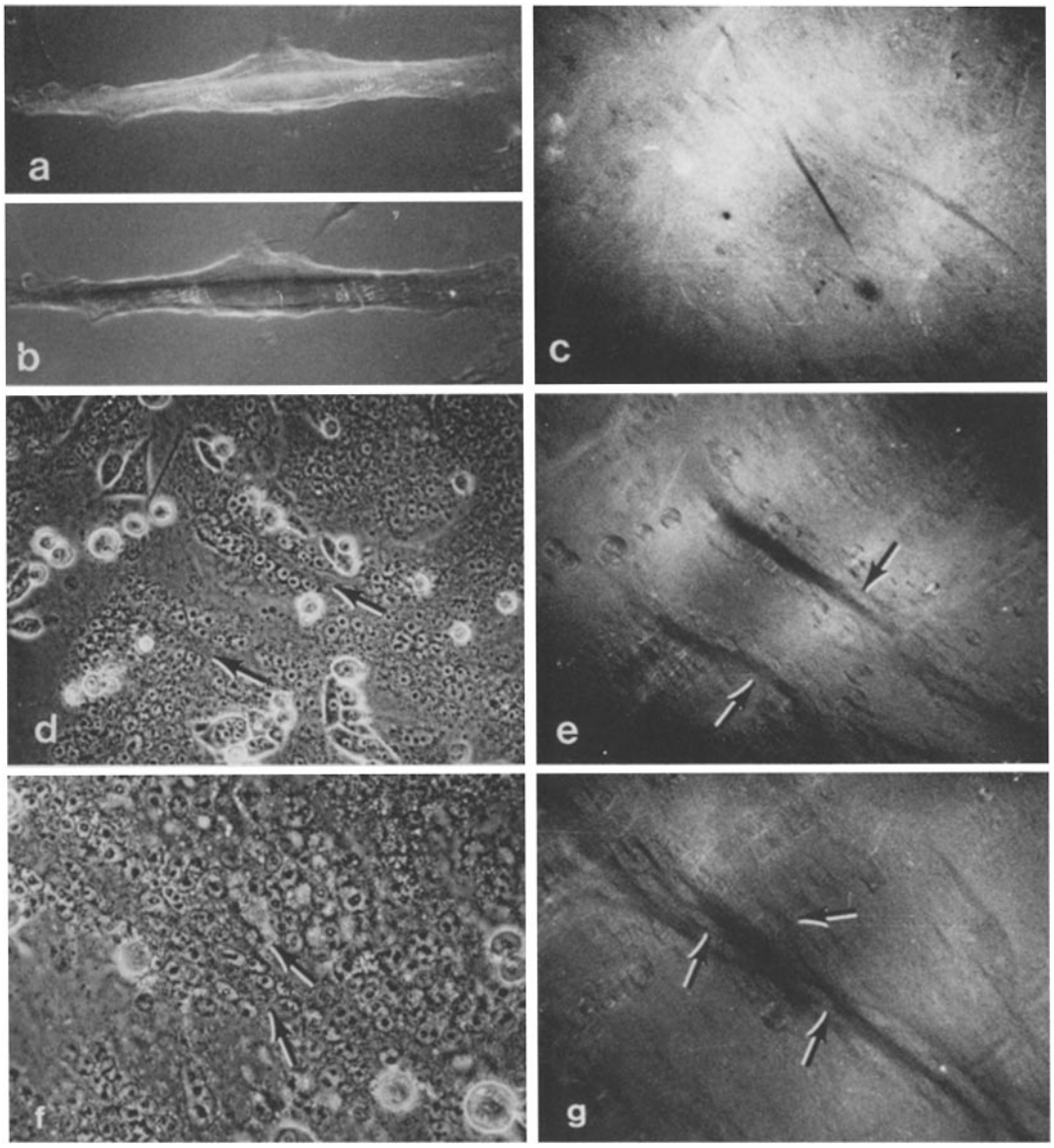

FIGURE 5 Changes in the intracellular birefringence pattern during nuclear movement and alignment in infected BHK21-F syncytia. Cytoplasmic birefringence was observed by polarized-light optics at high (*a-b*) and low (*c-g*) magnification. Infected cultures were incubated overnight at 33°C and then shifted to 39.5°C. Observations were made at various times after temperature shift. (*a* and *b*) Intracellular birefringence in a single BHK21-F cell. The two micrographs were taken at opposite compensator settings. × 1,200. (*c*) Birefringence pattern in BHK21-F syncytia 1 h after temperature shift. × 170. (*d*) Phase-contrast micrograph of the same area shown in *e*. Note the beginning of nuclear alignment in the area immediately outside the birefringent bands indicated in *e* (arrows). × 170. (*e*) Two large bands of intracellular birefringence (arrows) seen 2 h after temperature shift. × 170. (*f*) Phase-contrast micrograph of the same area shown in *g*. Note the parallel alignment of nuclei in the area of large birefringent bands. × 280. (*g*) Large bands of intracellular birefringence (arrows) 4 h after temperature shift. × 280.

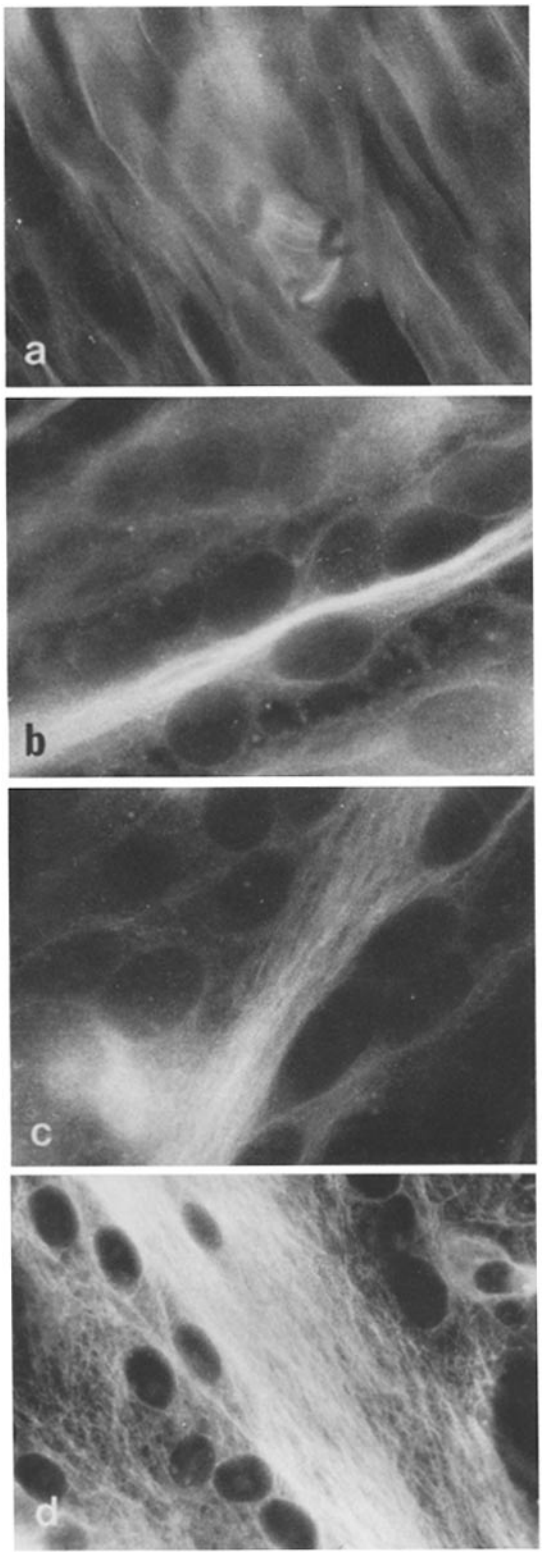

nuclear migration, and alignment was completed in 4–6 h. When observed with polarized-light optics at high magnification, single BHK21-F cells exhibited a positive birefringence along their long axes, which is usually contributed by the linear organization of microtubules and 10-nm filaments (19, 25, 54; Fig. 5 *a* and *b*). Almost immediately after shift to 39.5°C, fusion proceeded rapidly and positive birefringence could be easily observed in the cytoplasm at low magnification (Fig. 5 *c*). However, at this time only a few nuclei were aligned in parallel rows. As fusion progressed and the nuclei continued to become oriented in parallel rows, positive birefringent streaks of greater size were observed between the rows (Fig. 5 *d* and *e*). By 4 h after temperature shift, most of the nuclei were aligned in tightly packed parallel rows, and the birefringent streaks appeared very prominent and formed parallel arrays between aligned nuclei (25; Fig. 5 *f* and *g*).

The evolution of microtubule bundles during cell fusion and nuclear migration was also studied by immunofluorescence microscopy. The tubulin-staining patterns in infected cultures at 0.5, 1, 2, and 4 h after temperature shift are demonstrated in Fig. 6 *a–d*, respectively. As the cells fused into syncytia, microtubules usually assembled into a few small parallel-aligned bundles (Fig. 6 *a* and *b*). As the size of the syncytium increased during fusion, so did the size of the microtubule bundles (Fig. 6 *c*). Upon completion of fusion and nuclear migration, giant microtubule bundles of several microns in width and length appeared in the syncytial cytoplasm (Fig. 6 *d*). The bundles of microtubules were often seen in parallel orientation with respect to one another.

The assembly and organization of microtubules and 10-nm filaments into large bundles in SV5-infected BHK21-F cells occurred at a rapid rate after shift from 33° to 39.5°C. Thus, it seemed

FIGURE 6 Immunofluorescence microscopy of microtubule bundle formation during nuclear movement and alignment in infected BHK21-F cells. Cultures were treated with tubulin antibody at various times after shift from 33° to 39.5°C. (*a*) 0.5 h after temperature shift. Note the discrete parallel distribution of microtubules in individual cells and the tripolar spindle formation. × 675. (*b*) 1 h after shift. Microtubule bundle formation has begun. × 800. (*c*) 2 h after shift. The microtubule bundles have increased in size. × 800. (*d*) 4 h after shift. A typical large microtubule bundle has formed in the syncytium and the aligned nuclei are seen. × 675.

likely that the pool of materials for the organization of these large fibrous bundles was already present in the cytoplasm. This was investigated by observing nuclear movement and microtubule and 10-nm filament assembly in the absence of continued protein synthesis. Cultures were incubated at 33°C for 10 h, and then cycloheximide (20 μg/ml) was added at the time of temperature shift from 33° to 39.5°C. Although protein synthesis (measured by the incorporation of [^{35}S]methionine into TCA-precipitable counts) was inhibited by 99% compared with untreated controls, fusion proceeded as usual. At the time of cycloheximide treatment, enough viral protein had been inserted in the cell membrane so that inhibition of protein synthesis did not interfere with cell fusion. Nuclear migration and alignment were not inhibited by cycloheximide. Fluorescence-microscope examinations revealed that the cycloheximide-treated syncytia contain large bundles of microtubules and 10-nm filament bundles in a distribution similar to that seen in untreated cells (Fig. 7 *a* and *b*),

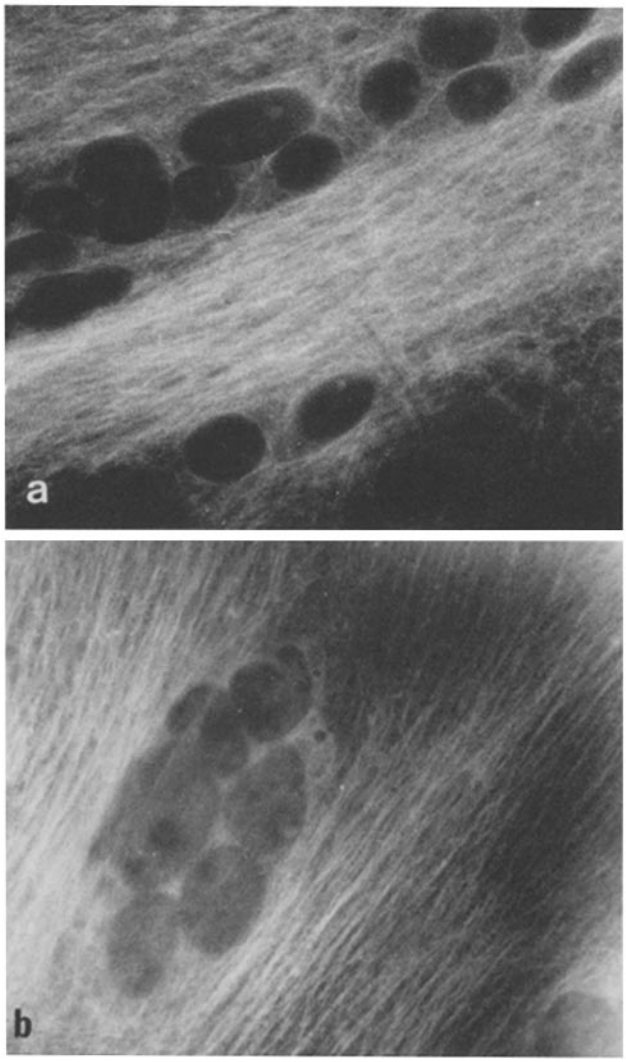

FIGURE 7 Formation of microtubule and 10-nm filament bundles in infected BHK21-F syncytia in the absence of protein synthesis. Cultures were incubated at 33°C and then shifted to 39.5°C. Cycloheximide (20 μg/ml) was added 1 h before temperature shift. The syncytia were treated with antiserum against tubulin (*a*) or against 10-nm filaments (*b*) 4 h after temperature shift. × 975.

and this observation indicated that the rapid assembly and organization of the two fibrous bundles did not require *de novo* protein synthesis.

Earlier studies reported that virus-induced syncytia derived from fibroblastic cells often have nuclei arranged in parallel rows, whereas syncytia derived from epitheloid cells contain round clusters of nuclei (24), and it was this difference that originally suggested that microtubules might play a role in the arrangement of nuclei in syncytia (25). A study of the morphogenesis of microtubule bundles in cultured epitheloid cells (CV-1) was undertaken to investigate further a possible correlation between microtubule organization and nuclear arrangement. Studies using antiserum against tubulin revealed that microtubules in CV-1 cells were organized in radiating arrays extending from the perinuclear region to the cell periphery (Fig. 8*a*). As the cells fused, the radiating microtubules merged and intertwined to form a criss-cross pattern around the nuclei (Fig. 8*b*). During fusion, large bundles of microtubules were also observed; however, these bundles, often converging together, were not arranged in parallel as seen in BHK21-F syncytia, and clusters of nuclei appeared to be randomly scattered among microtubule bundles. The nonparallel organization of microtubule bundles observed in SV5-infected CV-1 cells thus supports the cytoskeletal role for microtubules in nuclear alignment. Whereas the parallel arrangement of microtubule and 10-nm filament is accompanied by the parallel alignment of nuclei in BHK21-F syncytia, the failure of linear alignment of nuclei in CV-1 syncytia could result from a random distribution of microtubule bundles.

It is conceivable that microtubules and 10-nm filaments serve as cytoskeletal guides to direct nuclear movement, whereas the force for such movement could be produced by the actomyosin-like contractile system of microfilaments. To determine whether actinlike microfilament bundles are involved in the intracellular movements of nuclei, we have examined the possible relationship between aligned nuclei and the actin organization in the cytoplasm. Cytochalasin B (CB) at high concentration (20–50 μg/ml) was also used for disruption of functional microfilaments.

Actin-containing cytoplasmic fibers were visualized by indirect immunofluorescence microscopy using DNase I and antiserum against DNase I. Fig. 9*a* demonstrates the diffuse pattern of actin distribution between rows of nuclei. Such areas

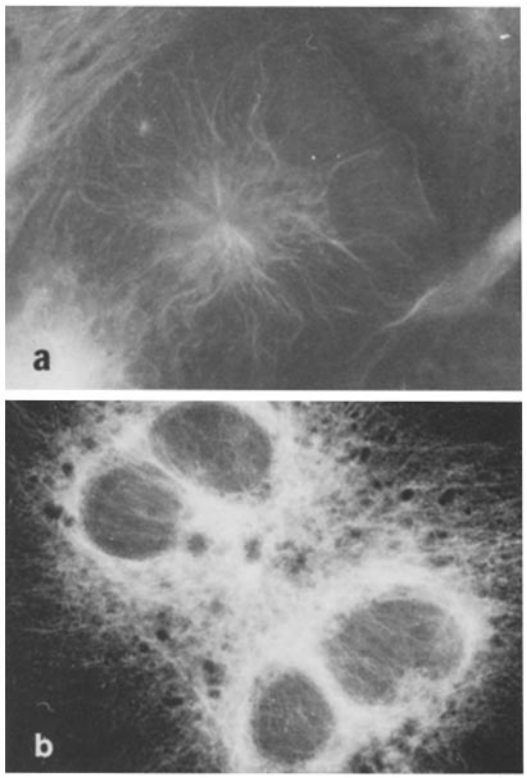

FIGURE 8 Immunofluorescence microscopy of microtubule bundle formation during the course of nuclear movement and aggregation in infected CV-1 cells. Cultures were treated with tubulin antibody at various times after temperature shift from 33° to 39.5°C. (*a*) The microtubules in single CV-1 cells are distributed radially. × 825. (*b*) A criss-cross pattern of microtubules in a syncytium containing four nuclei. × 800.

were shown above to contain bundles of microtubules and 10-nm filaments (Fig. 4). In contrast, the appearance of actin in organized fibers was found only in regions away from the linear rows of nuclei (Fig. 9*b*). In addition, randomly distributed fluorescent dots or granules were scattered throughout the cytoplasm. On comparison with controls (Fig. 9*c*), it would appear that these dots reflect the staining of actin. At present, the possible significance of actin in this granular organization is not known. Double staining with rhodamine-conjugated DNase I and antiserum against SV5 viral proteins reveals that some of the actin granules were also stained by SV5 antibody (data not shown), and may indicate a structural association of actin with SV5 viral proteins. A similar diffuse pattern of actin staining between aligned nuclei,

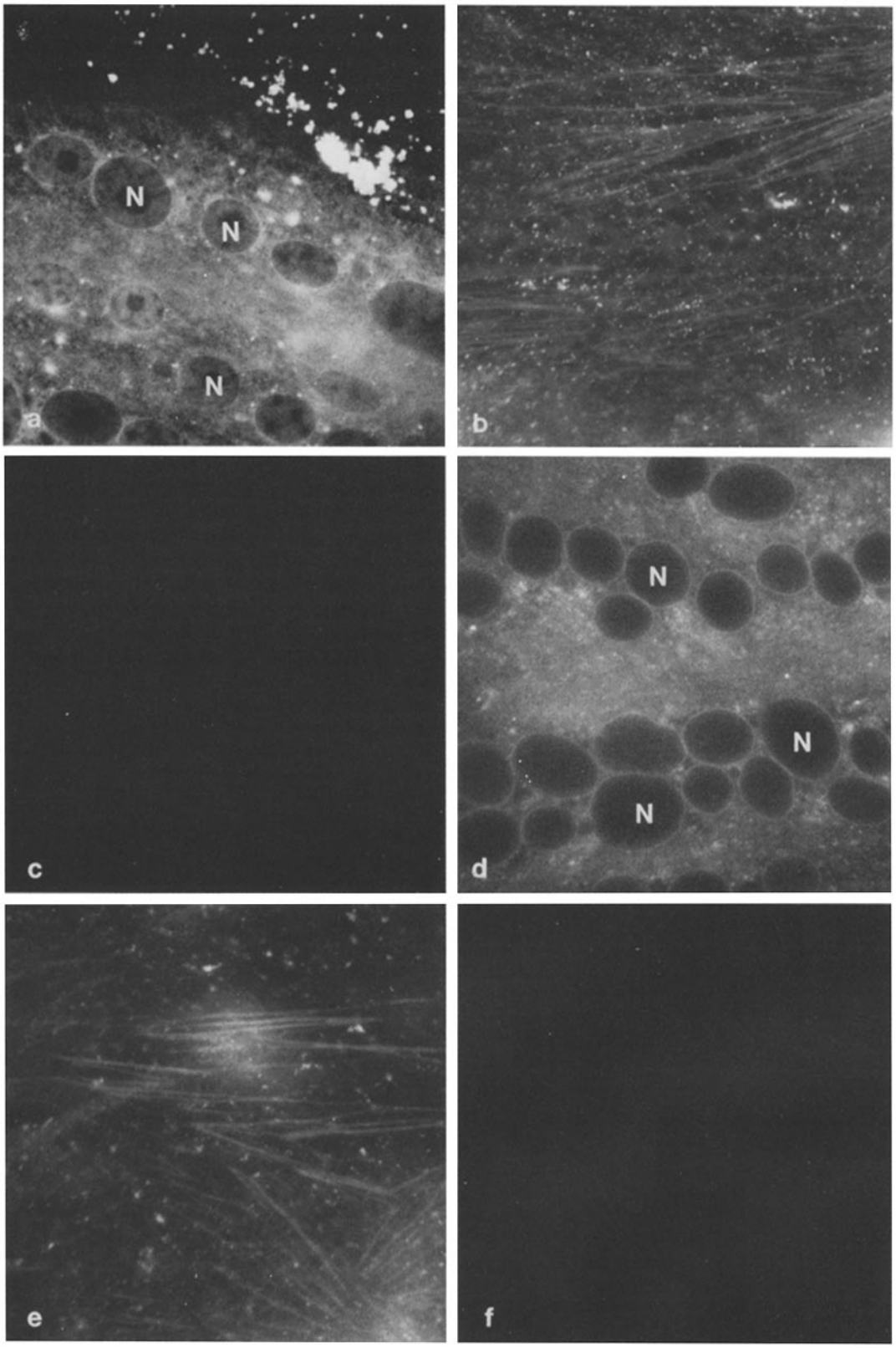
N
N
N
a
b
c
N
N
d
e
f

and fluorescent granules throughout the cytoplasm, was seen when the cells were reacted with fluorescein-avidin in combination with biotinyl-HMM (Fig. 9 *d-f*).

To avoid any possible effect of CB on virus adsorption, CB was added to the cells 2 h post-infection. The progress of cell fusion and nuclear motility was then monitored by time-lapse cinematography with phase-contrast optics. At 1–10 μg/ml, CB did not inhibit cell fusion or nuclear migration and alignment in SV5-infected BHK21-F cultures, and no significant morphological changes could be observed compared with untreated cultures (Fig. 10 *a* and *b*); normal movement and alignment of nuclei occurred. CB at 20–50 μg/ml, however, caused marked morphological changes in the infected syncytia (Fig. 10 *c*). Soon after treatment with CB, individual cells appeared to rise off the substrate and remained attached by only a few long filamentous processes. Time-lapse movies showed that as the processes of neighboring cells came in contact, fusion occurred and nuclei migrated through the long filamentous channels to the body of the syncytium. The cell fusion and nuclear movement continued, culminating in the formation of giant syncytium which remained attached to the substrate by numerous long filamentous processes (Fig. 10 *c*). Therefore, although a high dose of CB affects cell morphology, it does not inhibit cell fusion or nuclear movement. This finding suggests that microfilaments are not involved in the migratory activity of the nuclei.

Time-lapse movies, however, demonstrated that colchicine (10 μg/ml) did prevent nuclear movement along the slender channels in CB-induced syncytia. This result is consistent with the earlier observations in untreated infected cells which showed that disruption of microtubules by colchicine inhibited nuclear migration (25). Fluorescent staining with tubulin antiserum revealed that microtubules are indeed present in the long CB-induced projections. A large microtubule bundle usually extends from the main body of the syncytium to the tip of each projection (Fig. 11 *a*). Immunofluorescence studies with 10-nm filament antiserum demonstrated that the long filamentous projections also contain large numbers of 10-nm filaments (Fig. 11 *b*). Examination of ~200 syncytia showed that almost all of the filamentous projections contain bundles of microtubules and 10-nm filaments. Usually, the entire projection was filled with linearly packed tubules and filaments. Fig. 11 *c* illustrates a few nuclei that had been fixed while moving along a slender projection of a giant CB-induced syncytium. When this projection was stained with tubulin antiserum, microtubules were seen to surround the migratory nuclei (Fig. 11 *d*). Electron microscopy confirmed the immunofluorescence results (Fig. 12). Serial sections of the CB-induced long projections suggested that CB (20 μg/ml) had disrupted the organized bundle or meshwork form of microfilaments. Microtubules and 10-nm filament bundles, on the other hand, were observed to extend the entire length of the projection.

To obtain further evidence that CB at the high dosage of 20 μg had disrupted microfilaments, and to demonstrate that if microfilaments were associated with the aligned nuclei we could detect them, we examined serial sections of untreated cultures for the presence of microfilaments organized in the form of either bundles or meshworks. It has been shown in many previous studies that bundles composed of 40- to 70-Å filaments seen with electron microscopy are the stress fibers observed with phase-contrast optics, and that these fibers contain actin. The polymerized state of actin (F-actin) has been shown by "arrowhead" decoration on incubation with HMM. In our control samples (without CB treatment), large microfilament bundles were found in areas devoid of aligned nuclei (Fig. 13 *a*). In areas of aligned nuclei (cf. Fig. 4 *a*), one does not observe the presence of

FIGURE 9 SV5-infected BHK21-F syncytia treated with formaldehyde and acetone and subsequently stained with either DNase I and antiserum against DNase (*a-c*), or biotinyl-HMM and fluorescein-avidin (*d-f*) for visualization of actin organization. × 950. *a*) The diffuse immunofluorescence staining pattern of actin in an area of aligned nuclei (*N*). (*b*) Actin in fibrous form or granular organization in areas away from the nuclei. (*c*) The absence of fluorescence staining in the cytoplasm of a control preparation showing no staining when the DNase was mixed with rabbit skeletal muscle actin before incubation. (*d*) A diffuse staining pattern of actin similar to that seen in *a*, shown with labeled HMM. (*e*) An area similar to that in *b*, shown with labeled HMM. (*f*) Control cell treated with labeled HMM in the presence of sodium pyrophosphate.

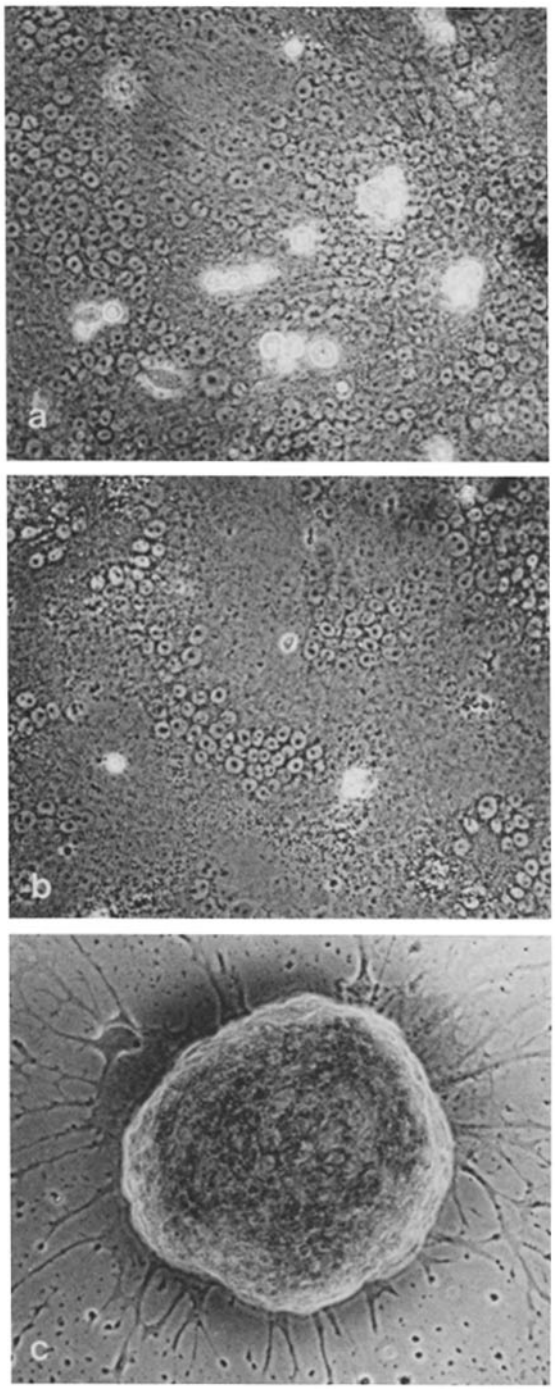

FIGURE 10 The effects of CB on nuclear movement and alignment in infected BHK21-F syncytia observed by time-lapse cinematography and phase-contrast optics. The cultures were infected with SV5 and subsequently treated with CB for 24 h at 37°C. × 191.4. (*a*) Untreated control. (*b*) 10 μg/ml CB. (*c*) 20 μg/ml CB. The syncytium has formed a large round body with long filamentous projections radiating from it.

microfilaments either in bundles or as a meshwork. Incubation of glycerinated syncytia with rabbit skeletal muscle HMM has shown that these microfilament bundles can be decorated, and may represent F-actinlike filaments (Fig. 13 *b*). Controls for HMM interaction with these actinlike fibers were carried out either by omitting HMM or by adding sodium pyrophosphate to prevent HMM binding to actin filaments, and in neither case were distinct arrowhead structures observed along microfilaments. When similar experiments with glycerination and HMM incubation were carried out with cells treated with 20 μg/ml CB, no HMM-decorated microfilaments were found, either in the main body of the syncytia or in the long filamentous projections. Examination of 20 different CB-treated syncytia yielded similar results. Therefore, the results indicate that CB at 20 μg/ml had disrupted most of the actin-containing microfilaments in BHK21-F cells; however, because of the difficulties in preserving actin filaments for electron microscopy, these observations do not exclude the possibility that some actin filaments remained in the cell.

DISCUSSION

Microtubules were shown previously to be necessary for the migration and alignment of nuclei in virus-induced syncytia (25). Using antibodies to cytoplasmic fibrous structures to study their distribution and morphogenesis, and the drug CB, we have confirmed and extended these earlier studies and obtained evidence that 10-nm filaments are also involved in nuclear movement and alignment. The formation of large bundles of microtubules and 10-nm filaments during the fusion of cells, and the migration and alignment of nuclei in rows parallel to these bundles, have suggested a mechanism for nuclear movement and positioning in the cell. In BHK21-F cells, microtubules are arranged in parallel arrays along the long axis of the cell, and the nucleus is usually located in the center of the cell surrounded by a network of microtubules. The parallel microtubules appear to originate from an organizing center containing a pair of centrioles. It is possible that, as two cells fuse, pairs of centrioles come together, and that the

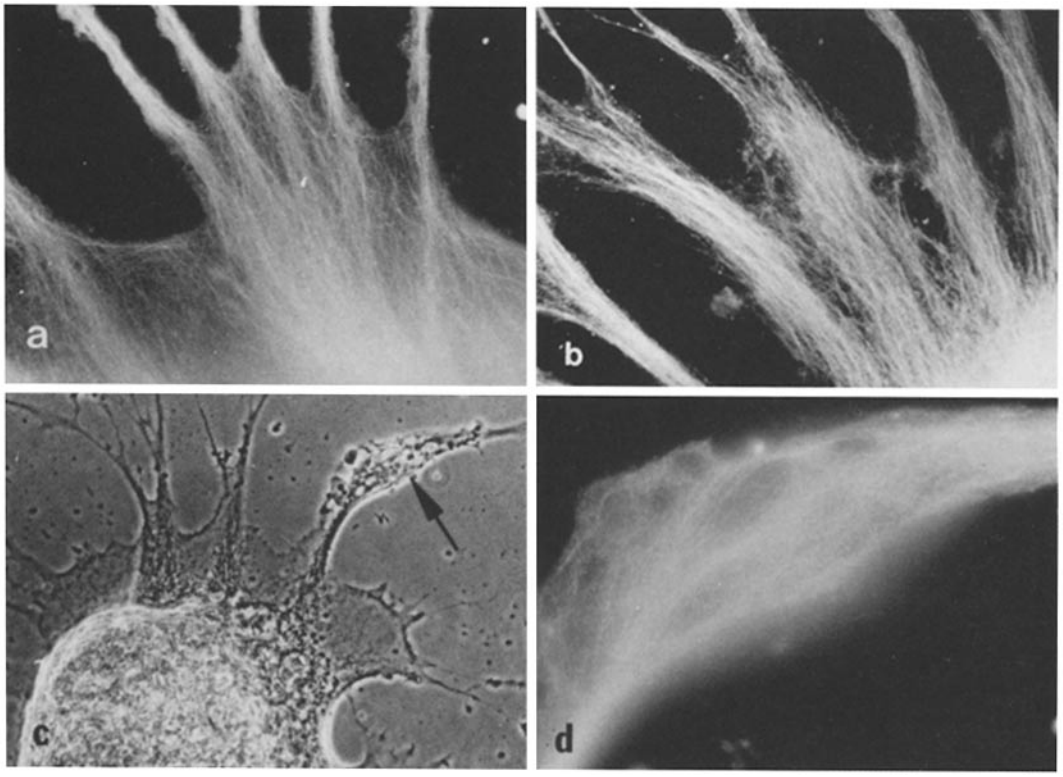

FIGURE 11 Immunofluorescence and phase-contrast microscopy of CB-induced projections. (*a*) Immunofluorescent staining pattern using tubulin antibody. Note the parallel array of microtubules. × 710. (*b*) Immunofluorescent staining pattern using 10-nm filament antibody. Note the parallel array of the 10-nm filaments. × 710. (*c*) Phase-contrast micrograph of migratory nuclei that had been fixed during their movement within a slender projection (arrow). × 185. (*d*) Immunofluorescence micrograph showing microtubules surrounding several migratory nuclei within the area indicated in *c*. × 710.

parallel microtubule networks which had surrounded the individual nuclei of the two cells merge into a small bundle which may then provide a tracklike structure along which the two nuclei are propelled and become linearly oriented. Thus, a continuing cycle of cell fusion, merging of centrioles, increase in microtubule bundles, and movement and alignment of nuclei may occur as the syncytium enlarges. The possibility that clusters of centrioles may serve as organizing centers for the formation of the large microtubule bundles is suggested by the earlier observation, in this laboratory (10, 25), of large clusters of centrioles in the syncytial cytoplasm, and we have again found such clusters in association with microtubule bundles.

Self-assembly of microtubules was first suggested by Inoué and co-workers (26, 27) and shown in vitro by Olmsted and Borisy (31, 32). Although detailed information on microtubule assembly in cultured cells is not available, it is thought that further organization of assembled microtubules into a definite pattern is a determinant of cell shape, is affected by transformation, and is involved in other tubule-associated functions (21). In the present system, microtubule assembly and organization into large bundles occurs to a striking degree, with large bundles forming that are many times the length of normal single cells. This occurs at a rapid rate; in as little as 4–6 h, a giant syncytium several centimeters in diameter can form, with the concomitant formation of large bundles of tubules and parallel arrangement of nuclei in clusters. The formation of such bundles occurs in the presence of cycloheximide, indicating that protein synthesis is not required.

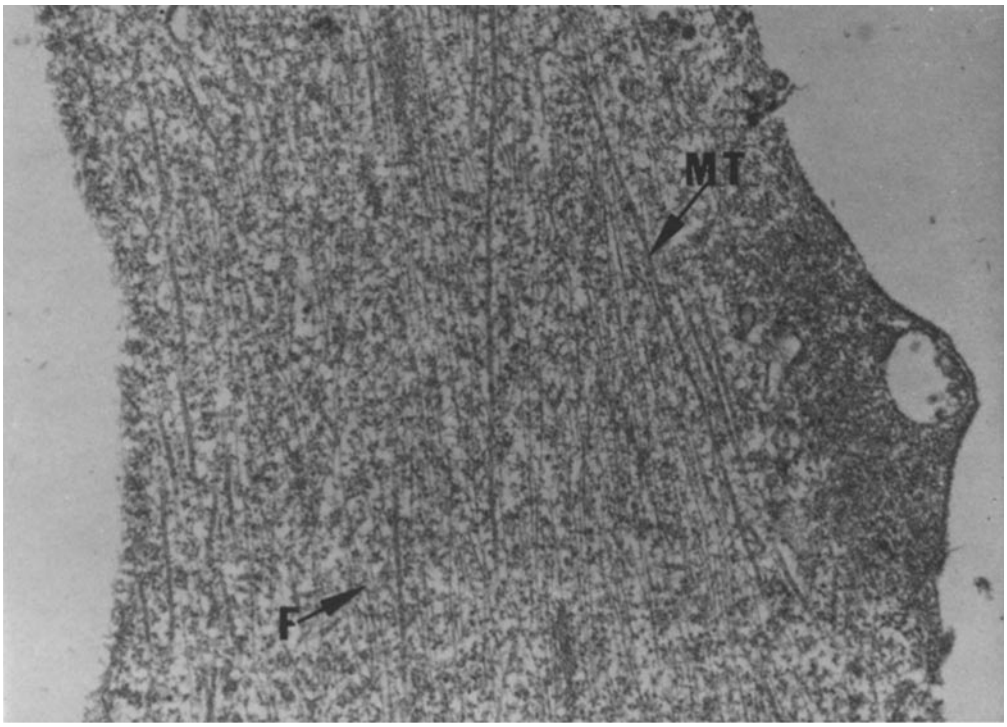

FIGURE 12 Electron micrograph of a CB-induced projection. Note the large number of microtubules (*MT*) and 10-nm filaments (*F*)., × 25,000.

Thus, the bundles are formed either by the condensation of preexisting polymerized tubules, or by the end addition of previously synthesized but unpolymerized subunits.

The magnitude of the assembly of microtubules in virus-induced syncytia raises the questions of the presence of microtubule-associated protein (MAP) (12) and τ-protein (11) in the large bundles, and whether the time and extent of tubulin assembly in our system can be regulated at different levels by divalent cation concentration (14), by the state of GTP binding (32), or by synthesis and phosphorylation of MAP (44, 45). The ability to study the rapid assembly of large bundles of microtubules under controlled conditions, such as described above, may provide a powerful means of investigating the regulation of this biologically important event.

Recently, 10-nm filaments have been characterized as a class of cytoplasmic fibers with unique antigenic and biochemical properties (20, 34, 43, 48, 49, 54, 57). They have been observed in the same orientation in the cytoplasm as microtubules (19, 25, 54), and are thought to depend on microtubules for their distribution in the cell (19). The present results indicate that parallel bundles of 10-nm filaments are found in abundance in the same areas of the syncytia as microtubules. During cell fusion, the morphogenesis of 10-nm filament bundles follows a pattern similar to that of microtubules; this process can occur in the presence of cycloheximide. Thus, as with microtubules, pools of precursors must be present in the cytoplasm, which can be assembled and organized into bundles without *de novo* protein synthesis. Earlier results from this laboratory (25) demonstrated that when microtubules were disrupted by colchicine treatment, 10-nm filaments were still present, but both nuclear movement and alignment were inhibited (25). Our preliminary results with immunofluorescence microscopy have shown that 10-nm filaments do not assemble into large bundles in the absence of microtubules. Furthermore, when colchicine (10 μg/ml) was added to CB-treated BHK21-F syncytia, not only did microtubule bundles disappear from the slender projections, but 10-nm filaments were also diminished. These observations support the suggestion that 10-

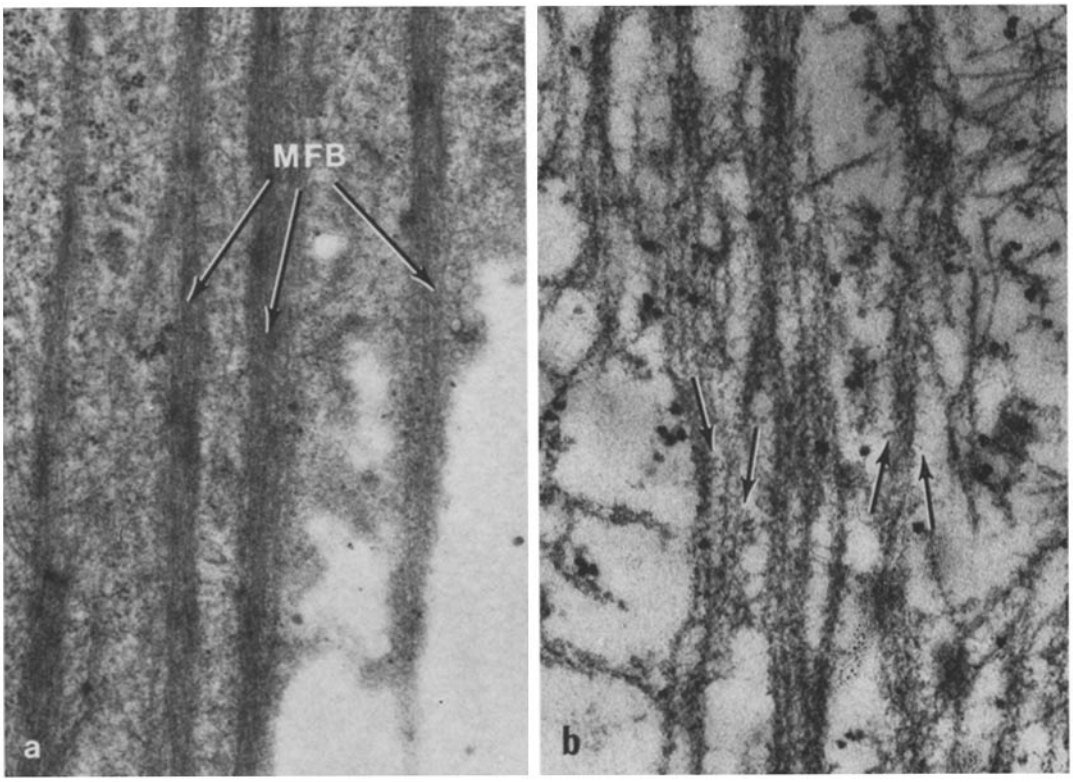

FIGURE 13 Electron micrographs showing typical microfilament bundles (*MFB*) and HMM-decorated microfilaments in SV5-infected BHK21-F syncytia. (*a*) A thin section taken just beneath the plasma membrane of the substrate side of an area of the syncytium away from the nuclear region. × 14,700. (*b*) A section from a similar area of a glycerinated syncytium. Actin-HMM complexes (arrows) in arrowhead configuration are present. × 58,450.

nm filaments may depend on microtubules for their distribution in the cytoplasm and further raise the possibility that 10-nm filaments may act in coordination with microtubules in the movement of nuclei through the syncytial cytoplasm. When the primary cytoskeleton contributed by microtubules is removed from the cytoplasm by colchicine, 10-nm filaments alone are not sufficient for the movement and linear arrangement of nuclei.

Actomyosin-containing microfilaments have long been thought of as generating the force for a variety of aspects of cell motility (1–5, 7, 18, 28, 41, 47, 55–57). Therefore, a reasonable hypothesis might have been that, in syncytia, microtubules and 10-nm filaments provided tracks for directing nuclear movement, and that microfilaments provided the motive force. On the other hand, our results with CB and the actin-staining patterns in syncytia provided no evidence for a major role for organized microfilaments in providing the force for nuclear migration. Although areas containing bundles of microtubules and 10-nm filaments can also be stained for actin, the diffuse pattern suggests that this type of cell motility seems to function without organized actin-containing microfilaments. In BHK21 cells, CB at concentrations as low as 0.5–1.0 μg/ml inhibited membrane ruffling, macropinocytosis, and cytokinesis but had no effect on the fine structure of microfilaments (19). However, at high concentrations (5–10 μg/ml), these processes were inhibited and microfilaments were disrupted (18, 19). Our results have clearly indicated that, at 20 μg/ml CB, BHK21-F cells and syncytia were depleted of almost all their microfilaments, but nuclear movement was not inhibited; nuclei moved along the CB-induced long processes which contained microtubules and 10-nm filaments. However, colchicine, which disrupts microtubules, prevented this nuclear move-

ment in the CB-treated syncytia. Thus, the movement of nuclei appears to result from the force generated in these processes by microtubules and/or 10-nm filaments. These results do not exclude the possiblity that actiin not organized into fibers or actomyosin-containing microfilaments could, under certain conditions, play a role in nuclear movement or positioning. For example, microfilaments could act as a dual force-generating mechanisms, and disruption could slow down movement but not prevent it. Careful analysis of the velocity of nuclear movement in CB-treated syncytia could shed light on this possibility.

The present results have suggested that, in addition to providing a framework which directs nuclear migration, the microtubules and 10-nm filaments may also take part in the system of force generation for the movement. The closely packed arrangement of tubules and 10-nm filaments into large bundles as demonstrated by electron microscopy suggest the possibility that a sliding motion, involving cross bridges, might exist. The electron-dense material of unknown composition interspersed between microtubules and 10-nm filaments and among the filaments themselves (Fig. 3 *b*) may represent such cross bridges. Similar morphological relationships between microtubules and 10-nm filaments have been reported in nerve axons (39, 40, 46) and in uninfected BHK21 cells (19, 54).

Force production involving highly organized microtubules has been proposed for movements including axonal transport (57), pigment migration (6), and saltatory motions of organelles in cultured cells (16, 23, 54). However, it is not known in our system whether microtubules alone, or both microtubules and 10-nm filaments, provide a force-generating system. Obviously, a better understanding of the function of 10-nm filaments, and the nature of their relationship with microtubules, is necessary. The lack of a specific agent which disrupts 10-nm filaments in mammalian cells has impeded such studies. Microinjection of specific antibody to various cellular fibrous components into viable cells may afford an approach to study 10-nm filament function.

We thank Dr. Robert D. Goldman for the antiserum for 10-nm filaments, Dr. Michael Heggeness for HMM and advice and assistance with these experiments, Dr. Allan R. Goldberg for helpful discussion, Cathleen O'Connell, Glenn Larsen, and Eric Carr for excellent technical assistance, and Chris Hellmann for printing of micrographs.

This research was supported by research grants PCM78-09091 from the National Science Foundation, AI-05600 from the National Institute of Allergy and Infectious Diseases, and BC-245 from the American Cancer Society. R. K. Cross was a Postdoctoral Fellow of the National Institute of Allergy and Infectious Diseases.

Received for publication 23 February 1979, and in revised form 27 July 1979.

REFERENCES

1. ABERCROMBIE, M., J. E. M. HEAYSMAN, and S. M. PEGRUM. 1970. The locomotion of fibroblasts in culture. I. Movements of the leading edge. *Exp. Cell Res.* **50**:393–398.
2. ALLÉRA, A., R. BECK, and K. E. WOHLFARTH-BOTTERMANN. 1971. Extensive fibrillar protoplasmic differentiations and their significance for protoplasmic streaming. VIII. Identification of the plasma filaments in *Physarium polycephalum* as F-actin by *in situ* binding of heavy meromyosin. *Cytobiologie.* **4**:436–449.
3. ALLISON, A. C. 1973. The role of microfilament and microtubules in cell movement, endocytosis and exocytosis. *Ciba Found. Symp.* **14**(new series):109–148.
4. ALLISON, A. C., P. DAVIES, and S. DEPETRIS. 1971. Role of contractile microfilaments in macrophage movement and endocytosis. *Nat. New Biol.* **232**:153–155.
5. ASH, J. F., and S. J. SINGER. 1976. Concanavalin A-induced transmembrane linkage of concanavalin A surface receptor to intracellular myosin-containing filaments. *Proc. Natl. Acad. Sci. U. S. A.* **73**:4575–4579.
6. BIKLE, D., L. G. TILNEY, and K. R. PORTER. 1966. Microtubules and pigment migration in the melanophores of *Fundulus heteroclitus L. Protoplasma.* **61**:322–345.
7. BLUEMINK, J. G. 1971. Cytokinesis and cytochalasin-induced furrow regression in the first-cleavage zygote of *Xenopus laevis. Z. Zellforsch. Mikrosk. Anat.* **121**:102–126.
8. CHANG, M. C., and R. D. GOLDMAN. 1973. The location of actin-like fibers in cultured neuroblastoma cells as revealed by HMM binding. *J. Cell Biol.* **57**:867–874.
9. CHOPPIN, P. W. 1964. Multiplication of a myxovirus (SV5) with minimal cytopathic effects and without interference. *Virology.* **23**:224–233.
10. COMPANS, R. W., K. V. HOLMES, S. DALES, and P. W. CHOPPIN. 1966. An electron microscopic study of moderate and virulent virus-cell interactions of the parainfluenza virus SV5. *Virology.* **30**:411–426.
11. CONNOLLY, J. A., V. J. KALNINS, D. W. CLEVELAND, and M. W. KIRSCHNER. 1977. Immunofluorescent staining of cytoplasmic and spindle microtubules in mouse fibroblasts with antibody to tau protein. *Proc. Natl. Acad. Sci. U. S. A.* **74**:2437–2440.
12. CONNOLLY, J. A., V. I. KALNINS, D. W. CLEVELAND, and M. W. KIRSCHNER. 1978. Intracellular localizations of the high molecular weight microtubule accessory protein by indirect immunofluorescence. *J. Cell Biol.* **76**:781–786.
13. D'ALISA, R. M., and E. L. GERSHEY. 1979. Characterization of a CV-1 cell cycle: I. Definition of a synchrony system. *Cell Tissue Kinet.* In press.
14. ERICKSON, H. P., and W. A. VOTER. 1976. Polycation-induced assembly of purified tubulin. *Proc. Natl. Acad. Sci. U. S. A.* **73**:2813–2817.
15. FORER, A., and O. BEHNKE. 1972. An actin-like component in spermatocytes of a crane fly (*Nephrotoma suturalis* Loew). I. The spindle. *Chromosoma (Berl.).* **39**:145–173.
16. FREED, J. J., and M. M. LEBOWITZ. 1970. The association of a class of saltatory movements with microtubules in cultured cells. *J. Cell Biol.* **45**:334–354.
17. GILBERT, D. 1978. 10 nm filaments. *Nature (Lond.).* **272**:577–578.
18. GOLDMAN, R. D., G. BERG, A. BUSHNELL, C.-M. CHANG, L. DICKERMAN, N. HOPKINS, M. L. MILLER, R. POLLACK, and E. WANG. 1973. Fibrillar systems in cell motility in locomotion of tissue cells. *Ciba Found. Symp.* **14**:83–107.
19. GOLDMAN, R. D., and D. KNIPE. 1973. Functions of cytoplasmic fibers in non-muscle cell motility. *Cold Spring Harbor Symp. Quant. Biol.* **37**: 523–534.
20. GORDON, W. E., A. BUSHNELL, and K. BURRIDGE. 1978. Characteriza-

tion of the intermediate (10 nm) filaments of cultured cells using an autoimmune rabbit antiserum. *Cell.* **13**:249–261.

21. HANAFUSA, H. 1977. Cell transformation by RNA tumor viruses. *In* Comprehensive Virology, Vol. 10. 401–483.
22. HEGGENESS, M. H., and J. F. ASH. 1977. Use of the avidin-biotin complex for the localization of actin and myosin with fluorescence microscopy. *J. Cell Biol.* **73**:783–788.
23. HEGGENESS, M. H., M. SIMON, and S. J. SINGER. 1978. Association of mitochondira with microtubules in cultured cells. *Proc. Natl. Acad. Sci. U. S. A.* **75**:3863–3866.
24. HOLMES, K. V., and P. W. CHOPPIN. 1966. On the role of the response of the cell membrane in determining virus virulence. Contrasting effect of the parainfluenza virus SV5 in two cell types. *J. Exp. Med.* **124**:501–522.
25. HOLMES, K. V., and P. W. CHOPPIN. 1968. On the role of microtubules in movement and alignment of nuclei in virus-induced syncytia. *J. Cell Biol.* **39**:526–543.
26. INOUÉ, S., J. FUSELER, E. SALMON, and G. W. ELLIS. 1975. Functional organization of mitotic microtubules: physical chemistry of the in vivo equilibrium system. *Biophys. J.* **15**:725–744.
27. INOUÉ, S., and H. RITTER, JR. 1975. Dynamics of mitotic spindle organization and functions. *In* Molecules and Cell Movement. S. Inoué and R. E. Stephens, editors. Raven Press, New York. 3–30.
28. KOMINICK, H., W. STOCKEM, and K. R. WOHLFARTH-BOTTERMANN. 1972. Cell motility mechanisms in protoplasmic streaming and amoeboid movement. *Fortschr. Zool.* **21**:1–74.
29. LOCKE, M., and N. KRISHNAN. 1971. Hot alcoholic phosphotungstic acid and uranyl acetate as routine stains for thick and thin sections. *J. Cell Biol.* **50**:550–557.
30. LUFT, J. H. 1961. Improvements in epoxy resin embedding method. *J. Biophys. Biochem. Cytol.* **9**:409–414.
31. OLMSTED, J. B., and G. G. BORISY. 1973. Microtubules. *Annu. Rev. Biochem.* **42**:507.
32. OLMSTED, J. B., AND G. G. BORISY. 1975. Ionic and nucleotide requirements for microtubule polymerization in vitro. *Biochemistry.* **14**:2996–3005.
33. ORR, T. S. C., D. E. HALL, and A. C. ALLISON. 1972. Role of contractile microfilaments in the release of histamine from mast cells. *Nature (Lond.).* **236**:350–351.
34. OSBORN, M. W., W. FRANKE, and K. WEBER. 1977. Visualization of a system of filaments 7–10 nm thick in cultured cells of an epitheloid line (ptk2) by immunofluorescence microscopy. *Proc. Natl. Acad. Sci. U. S. A.* **74**:2490–2494.
35. PETERS, A., S. L. PALAY, and H. WEBSTER. 1970. The Fine Structure of the Nervous System. Harper & Row, Publishers, Inc., New York. 198.
36. POLLARD, T. D., and S. ITO. 1970. Cytoplasmic filaments of *Amoeba proteus* I. The role of filaments in consistency changes and movements. *J. Cell Biol.* **46**:267–289.
37. POLLARD, T. D., E. SHELTON, R. WEIHING, and E. KORN. 1970. Ultrastructural characterization of F-actin from *Acanthamoeba Castellani* and identification of cytoplasmic filaments as F-actin by reaction with rabbit heavy meromyosin. *J. Mol. Biol.* **50**:91–97.
38. REYNOLDS, R. 1963. The use of lead citrate at high pH as an electron-opaque stain in electron microscopy. *J. Cell Biol.* **17**:208–212.
39. SCHMITT, F. O. 1968. The molecular biology of neuronal fibrous proteins. *Neurosci. Res. Program Bull.* **6**:119–144.
40. SCHMITT, F. O. 1968. Fibrous proteins-neuronal organelles. *Proc. Natl. Acad. Sci. U. S. A.* **60**:1092–1104.
41. SCHROEDER, T. E. 1968. Cytokinesis: filaments in the cleavage furrow. *Exp. Cell Res.* **53**:272–276.
42. SHELANSKI, M. L., and E. W. TAYLOR. 1967. Isolation of a protein subunit from microtubules. *J. Cell Biol.* **34**:549–554.
43. SHELANSKI, M. L., S. H. YEN, and V. M. LEE. 1976. Neurofilaments and glial filaments. *In* Cell Motility. R. Goldman, T. Pollard, and J. Rosenbaum, editors. Cold Spring Harbor Laboratory, Cold Spring Harbor, N. Y. 1007–1020.
44. SLOBODA, R. D., W. L. DENTLER, R. A. BLOODGOOD, B. R. TELZER, S. GRANETT, and J. L. ROSENBAUM. 1976. Microtubule-associated proteins (MAPs) and the assembly of microtubules in vitro. Cold Spring Harbor Symposium on Cell Motility. 1171–1212.
45. SLOBODA, R. D., W. L. DENTLER, and J. L. ROSENBAUM. 1976. Microtubule-association proteins and the stimulation of tubulin assembly in vitro. *Biochemistry.* **15**:4497–4505.
46. SMITH, D. S., V. JALFORS, and B. F. CAMERON. 1975. Morphological evidence for the participation of microtubules in axonal transport. *Ann. N. Y. Acad. Sci.* **253**:472–506.
47. SPOONER, B. S., K. M. YAMADA, and N. K. WESSELS. 1971. Microfilaments and cell locomotion. *J. Cell Biol.* **49**:595–613.
48. STARGER, J. M., W. E. BROWN, A. E. GOLDMAN, and R. D. GOLDMAN. 1978. Biochemical and immunological analysis of rapidly purified 10-nm filaments from baby hamster kidney (BHK-21) cells. *J. Cell Biol.* **78**:93–109.
49. STARGER, J. M., and R. D. GOLDMAN. 1977. Isolation and preliminary characterization of 10 nm filaments from baby hamster kidney (BHK-21) cells. *Proc. Natl. Acad. Sci. U. S. A.* **74**:2422–2426.
50. STOKER, M. G. P., and I. MACPHERSON. 1964. Syrian hamster fibroblast cell line BHK-21 and its derivatives. *Nature (Lond.).* **203**:1355–1356.
51. SZENT-GYÖRGYI, A. 1951. Chemistry of Muscular Contraction, 2nd edition. Academic Press, Inc., New York. 146–148.
52. WANG, E., R. K. CROSS, and P. W. CHOPPIN. 1978. Possible roles at microtubules and 10-nm filaments in intracellular movements in cells infected with a paramyxovirus. *J. Cell Biol.* **79**(2, Pt. 2):303*a*. (Abstr.).
53. WANG, E., and A. R. GOLDBERG. 1978. Binding of deoxyribonuclease I to actin: a new way to visualize microfilament bundles in nonmuscle cells. *J. Histochem. Cytochem.* **26**:745–749.
54. WANG, E., and R. D. GOLDMAN. 1978. Functions of cytoplasmic fibers in intracellular movements in BHK-21 cells. *J. Cell Biol.* **79**:708–726.
55. WESSELLS, N. K., B. S. SPOONER, J. S. ASH, M. O. BRADLEY, M. A. LUDUENA, E. L. TAYLOR, J. T. WRENN, and K. M. YAMADA. 1971. Microfilaments in cellular and developmental processes. *Science (Wash. D. C.).* **171**:135–143.
56. WESSELLS, N. K., B. S. SPOONER, and M. A. LUDENA. 1973. Surface movements, microfilaments and cell locomotion. *Ciba Found. Symp.* **14**(new series):53–82.
57. WUERKER, R. B., and J. B. KIRKPATRICK. 1972. Neuronal microtubules, neurofilaments and microfilaments. *Int. Rev. Cytol.* **33**:45–75.